Electronic Supplementary Information

Bridging-patching *c*-pore with Tetratrifluoroacetate in A *csq*-type Mesoporous Zr-MOF with Different Crystal Dimensions: Cycling stability And Adsorption Kinetics For In-door Humidity Control

*Hao Lin, Huiying Lin, Mingxing Zhang, Yingpeng Jiang, Yuhang Liu, Liting Du, Zhiyong Lu**

Table of contents

1. Materials and General Methods

2. Synthesis of NU-1008 analogues

3. Water-soaking Treatment

4. Characterizations for NU-1008 analogues

5. Characterizations for NU-1008-TFS with different crystal dimensions

6. References

1. Materials and General Methods

Materials. All reagents were obtained from commercial vendors and, unless otherwise noted, were used without further purification.

Physical Methods and Instrumentation.

N_2 isotherms were collected on an Anton Paar Autosorb 6100 instruments at 77 K. Before N_2 adsorption, MOF samples were treated by thermal-vacuo activation at 120 °C for 12h.

Water isotherms were collected on an Anton Paar Autosorb 6100 instruments at 298 K. The steam generation condition is 308 K, and the water adsorption test is conducted at 298 K. Before water-vapor adsorption, MOF samples were treated by thermal-vacuo activation at 120 °C for 12h.

Water adsorption kinetics tests. Dynamic water vapor adsorption and desorption experiments were collected under constant humidified airflow through BSD-VVS&DVS intelligent gravimetric analyzer (Beishide Instrument Technology (Beijing) Co., Ltd) with a mass inaccuracy is ±0.001 mg. It was automatically controlled to accurately regulate the temperature (5 to 300 °C) and water vapor pressure (1 to 95% RH). The adsorption measurements on NU-1008 analogues were carried out at 298 K and 80% relative humidity, while desorption measurements were conducted at 338 K and 30% relative humidity, with a maximum equilibrium time of 3 hours. Prior to tests, all samples underwent vacuum thermal activation at 120 °C for 10 hours to remove the solvent. Nitrogen (99.999%) were applied as the flowing gas to carry water vapor.

^{1}H NMR spectroscopy. Samples digestion was carried out in two ways: 1) 2 mg of MOF was placed into a 1.5 mL vial. About 3 to 4 drops of 0.1 M NaOD in D_2O digestion medium was then added to the vials. The vials were capped and inverted 2 or 3 times before sonicating for 30 min. To the mixture, 17 drops of D_2O were added. Then the mixture was centrifuged and the clear supernatant solution was transferred to an NMR tube; 2) 2 mg of MOF was placed into a 1.5 mL vial. About 3 to 4 drops of D_2SO_4 was then added. The vials were capped and sonicating for 30 min. To the mixture, 20 drops of d_6-DMSO were added. Then the clear supernatant solution was transferred to an NMR tube. ^{1}H NMR spectra were recorded with a JNM-ECZ401S NMR spectrometer (400 MHz; 8 scans).

^{19}F NMR spectroscopy. 2 mg of MOF and 1 mg Internal standard (1,4-dibromo-2,5-bis(trifluoromethyl)benzene) was placed into a 1.5 mL vial. About 3 to 4 drops of D_2SO_4 was then added.

The vials were capped and sonicating for 30 min. To the mixture, 20 drops of d_6-DMSO were added. Then the clear supernatant solution was transferred to an NMR tube. ^{19}F NMR spectra were recorded with a JNM-ECZ401S NMR spectrometer (400 MHz; 16 scans).

Fourier transform infrared spectrometer (FT-IR) spectra were recorded on a Nicolet iS10 FT-IR spectrometer equipped with an DTGS detector. Samples diluted in KBr were measured with a KBr background (samples prepared in atmosphere). The spectra were collected at 4 cm^{-1} resolution and 16 scans were averaged over the spectral window of 400-4000 cm^{-1}.

Power X-ray diffraction (PXRD) was collected on a Bruker D8 ADVANCE X-ray diffractometer with Cu/ Kα radiation, and the data collecting range (2θ) was set between +2°~+20°. Simulated powder patterns from single-crystal X-ray diffraction data were generated using Mercury 1.4.2 software.

Thermo-gravimetric analysis (TGA) was performed using a NETZSCH STA 2500 under a nitrogen atmosphere (purge gas: 20 mL min^{-1}; protective gas: 50 mL min^{-1}). The sample was heated from 30 °C to 800 °C at a rate of 10 °C min^{-1}.

Single-crystal X-ray diffraction (SCXRD) were obtained from Rigaku XtaLAB Synergy-DW single crystal diffractometer equipped with graphite-monochromatic Cu/Kα radiation (λ = 1.54184 Å) at 100 K / 300K. The structures were solved by intrinsic phasing (SHELXT) methods and refined with full-matrix least squares technique using the SHELXL package. Non-hydrogen atoms were refined with anisotropic displacement parameters during the final cycles. Organic hydrogen atoms were placed in calculated positions with isotropic displacement parameters set to 1.2 × U_{eq} of the attached atom. The unit cell includes a large region of disordered solvent molecules, which could not be modeled as discrete atomic sites. We employed PLATON/SQUEEZE to calculate the diffraction contribution of the solvent molecules and thereby, to produce a set of solvent-free diffraction intensities; structures were then refined again using the data generated. Crystallographic data for NU-1008, NU-1008-FUM, NU-1008-TFA, and NU-1008-TFS crystal structure in CIF format have been deposited in the Cambridge Crystallographic Data Centre (CCDC) under deposition numbers CCDC-2513590 and 2501574-2501576. The data can be obtained free of charge via www.ccdc.cam.ac.uk/data_request/cif (or from the Cambridge Crystallographic Data Centre, 12 Union Road, Cambridge CB2 1EZ, U.K.). Detailed crystal data and structure refinements for NU-1008, NU-1008-FUM, NU-1008-TFA and NU-1008-TFS are listed in Tables S1.

Table S1. Crystal data and structure refinement for **NU-1008-analogue**

Compound	**NU-1008**	**NU-1008-FUM**	**NU-1008-TFA**	**NU-1008-TFS**
CCDC number	2513590	2501574	2501575	2501576
Empirical formula	$C_{35}H_{17}Br_2O_{16}Zr_3$	$C_{36}H_{17}O_{16}Br_2Zr_3$	$C_{36}H_{18}O_{16}F_3Br_2Zr_3$	$C_{38}H_{18}O_{18}F_4Br_2Zr_3$
Formula weight	1126.95	1138.96	1196.98	1271.98
Temperature / *K*	100.15	100.00(10)	300.7(6)	302(2)
Crystal system	hexagonal	hexagonal	hexagonal	hexagonal
Space group	*P6/mmm*	*P6/mmm*	*P6/mmm*	*P6/mmm*
a/Å	40.5006(3)	40.3896(3)	40.3896(3)	40.2180(9)
b/Å	40.5006(3)	40.3896(3)	40.3896(3)	40.2180(9)
c/Å	11.42740(10)	11.5335(10)	11.5335(10)	11.6882(2)
α/°	90	90	90	90
β/°	90	90	90	90
γ/°	120	120	120	120
Volume/Å³	16233.1(3)	16294.1(3)	16294.1(3)	16372.7(8)
Z	6	6	6	6
ρ_{calc} /g cm^{-3}	0.692	0.682	0.732	0.774
μ/mm^{-1}	3.420	3.339	3.465	3.496
F(000)	3270.0	3306.0	3474.0	3696.0
Radiation	Cu/Kα (λ = 1.54184)	Cu/Kα (λ = 1.54184)	Cu/Kα (λ = 1.54184)	Cu/Kα (λ = 1.54184)
2Θ range for data collection/°	4.364 to 154.86	4.524 to 154.782	4.376 to 148.99	4.394 to 154.828
Index ranges	-39⩽h⩽50, -50⩽k⩽50, -13⩽l⩽9	-48⩽h⩽49, -48⩽k⩽49, -11⩽l⩽15	-48⩽h⩽50, -50⩽k⩽50, -12⩽l⩽14	-47⩽h⩽50, -49⩽k⩽50, -13⩽l⩽14
Reflections collected	104532	106002	103809	102036
Independent reflections	6610[R_{int}=0.0873, R_{sigma}=0.0319]	6610[R_{int}=0.0873, R_{sigma}=0.0319]	6097[R_{int}=0.08, R_{sigma}=0.0267]	6319[R_{int}=0.0654, R_{sigma}=0.0236]
Data/restraints/parameters	6384/18/141	6610/9/147	6266/48/154	6319/46/168
Goodness-of-fit on F^2	1.034	1.178	1.231	1.192
Final R indexes [I>=2σ (I)]	R_1=0.0355, wR_2=0.0944	R_1=0.0457, wR_2=0.1424	R_1=0.0457, wR_2=0.1424	R_1=0.0606, wR_2=0.1970
Final R indexes [all data]	R_1=0.0394, wR_2=0.0965	R_1=0.0457, wR_2=0.1424	R_1=0.0511, wR_2=0.1476	R_1=0.0646, wR_2=0.2035
Largest diff. peak/hole/eÅ^{-3}	1.19/-1.83	1.30/-1.08	1.90/-1.24	3.23/-2.22

Scanning electron micrographs (SEM) images were taken using a Quanta FEG 250. Evenly distribute the sample on the conductive adhesive and spray metallic silver on the surface of the conductive adhesive before testing.

2. Synthesis of NU-1008 analogues

Synthesis of NU-1008-O (acorn-shaped powder**).** 66.4 mg $ZrO(NO_3)_2 \cdot 6H_2O$ (0.267 mmol) was dissolved in a mixed solvent of 1.5 mL DMF and 1 mL formic acid. After ultrasonic dissolution, it was heated at 80 °C for 1 hour. 38.2 mg $H_4TCPB\text{-}Br_2$ (0.0523 mmol) was dissolved in 1.5 mL of DMF and heated at 80 °C for 1 hour to ensure complete dissolution. After the two solutions have cooled to room temperature, transfer the ligand solution to the Zr_6 cluster solution. Sealed reaction system, constant temperature reaction at 100 °C for 15-16 hours. After the reaction was completed, the products were obtained through centrifugal separation and washed successively with DMF (5 mL×3) and acetone (5 mL×3). Then the product was soaked in acetone for 12 hours and washed with acetone three times again. The product was first vacuum dried at 65 °C, and finally vacuum activated at 120 °C for 12 hours to obtain the activated NU-1008-O sample. Except for NU-1008-O-TFS, NU-1008-I-TFS，NU-1008-II-TFS and NU-1008-SC-TFS, the NU-1008 analogues all are synthesized by NU-1008-O.

Synthesis of NU-1008-I (short-rod-shaped powder**).** In a 7.5 mL sample bottle, 7.42 mg $H_4TCPB\text{-}Br_2$ (0.01 mmol) and 9.32 mg $ZrCl_4$ (0.04 mmol) were added to 2 mL DMF, and 0.75 mL formic acid was added and ultrasonically dissolved. Seal the mixed solution and place it in an environment of 120 °C for 24 hours of reaction. After the system cools to room temperature, the solid product is obtained through centrifugal separation. Wash successively with DMF (5 mL×3) and acetone (5 mL×3), and then soak the product in acetone for 12 hours. After washing with acetone three times again, the solid was collected and vacuum-dried at 65 °C, and finally vacuum activated at 120 °C for 12 hours to obtain the activated NU-1008-I sample.

Synthesis of NU-1008-II (long-rod-shaped powder**).** 9.66 mg of $H_4TCPB\text{-}Br_2$ (0.0130 mmol) was added to 5 ml of DEF and ultrasonically. 18.7 mg of $ZrCl_4$ (0.08 mmol) was added to 5 ml of DEF and 0.3 ml of formic acid was added. After ultrasonically treatment, it was placed in an oven at 80 °C for 1 hour. After cooling to room temperature, mix the solution, add 4.5 mL of formic acid, ultrasonicate, heat at 120 °C for 5 days, and then volatilize at 120 °C for 5 days. Wash successively with DMF (5 mL×3) and acetone (5 mL×3), and then soak the product in acetone for 12 hours. After washing with acetone three times again, the solid was collected and vacuum-dried at 65 °C, and finally vacuum activated at 120 °C for 12 hours to obtain the activated NU-1008-II sample.

Synthesis of NU-1008- SC (bulk single crystal**).** 9.66 mg of $H_4TCPB\text{-}Br_2$ (0.0130 mmol) was added to 5 ml of DEF and ultrasonically. 18.7 mg of $ZrCl_4$ (0.08 mmol) was added to 5 ml of DEF and 0.3 ml of formic acid was added. After ultrasonically treatment, it was placed in an oven at 80 °C for 1 hour. After cooling to room temperature, mix the solution, add 4.5 mL of formic acid, ultrasonicate, heat at 120 °C for 5 days, and then volatilize at 120 °C for 7 days. Wash successively with DMF (5 mL×3) and acetone (5 mL×3), and then soak the product in acetone for 12 hours. After washing with acetone three times again, the solid was collected and vacuum-dried at 65 °C, and finally vacuum activated at 120 °C for 12 hours to obtain the activated NU-1008-SC sample.

Preparation of NU-1008-FUM. 30 mg NU-1008-O was added to 4.5 mL DMF, then 25.5 mg of fumaric acid (0.220 mmol) was added. After ultrasonic treatment, it was placed in an oven at 75 °C for 24 hours. Wash successively with 65 °C DMF (5 mL×3) for one hour each time. Then add 0.125 mL of 2 M HCl and 3 mL of DMF and place in an oven at 100 °C for 18 hours. Wash successively with DMF (5 mL×3) and acetone (5 mL×3), and then soak the product in acetone for 12 hours. After washing with acetone three times again, the solid was collected and vacuum-dried at 65 °C, and finally vacuum activated at 120 °C for 12 hours to obtain the activated NU-1008-FUM sample.

Preparation of NU-1008-TFA. 30 mg NU-1008-O was added to 3 mL DMF, then 15 μL of trifluoroacetic acid (0.196 mmol) was added. After ultrasonic treatment, it was placed in an oven at 75 °C for 24 hours. Wash successively with 65 °C DMF (5 mL×3) and acetone (5 mL×3) for one hour each time, and then soak the product in acetone for 12 hours. After washing with acetone three times again, the solid was collected and vacuum-dried at 65 °C, and finally vacuum activated at 120 °C for 12 hours to obtain the activated NU-1008-TFA sample.

Preparation of NU-1008-O-TFS, NU-1008-I-TFS, NU-1008-II-TFS and NU-1008-SC-TFS. 30 mg NU-1008-O, NU-1008-I, NU-1008-II and NU-1008-SC was added to 15 mL DMF separately, then 45 mg of tetrafluorosuccinic acid (0.237 mmol) was added. After ultrasonic treatment, it was placed in an oven at 75 °C for 24 hours. Wash successively with 65 °C DMF (5 mL×3) for one hour each time. Then add 0.125 mL of 2 M HCl and 3 mL of DMF and place in an oven at 100°C for 18 hours. Wash successively with DMF (5 mL×3) and acetone (5 mL×3), and then soak the product in acetone for 12 hours. After washing with acetone three times again, the solid was collected and vacuum-dried at 65 °C for 1h, and finally vacuum activated at 120 °C for 12 hours to obtain the activated NU-1008-O-TFS, NU-1008-I-TFS, NU-1008-II-TFS and NU-1008-SC-TFS sample.

3. Water-soaking Treatment

The following procedure was uniformly applied to all NU-1008 analogues. For each analogue, 10 mg of the material was immersed in water, which was replaced every eight hours (three times per day). After soaking for one, two, and three days, respectively, 2 mg aliquots were collected for subsequent ^{1}H NMR sample preparation. Prior to NMR analysis, each aliquot was washed three times with 3 mL of acetone (1 hour per wash) and then dried in an oven at 65 °C. The dried sample was transferred into a 1.5 mL vial, to which approximately 3–4 drops of a 0.1 M NaOD/D_2O (or D_2SO_4 for acidic digestion) were added. The vial was capped, inverted two or three times, and sonicated for 30 minutes. Subsequently, 17 drops of D_2O (or d_6-DMSO for acidic digestion) were added, and the mixture was centrifuged. The resulting clear supernatant was then transferred to an NMR tube for analysis. This protocol ensures consistent sample treatment across all analogues.

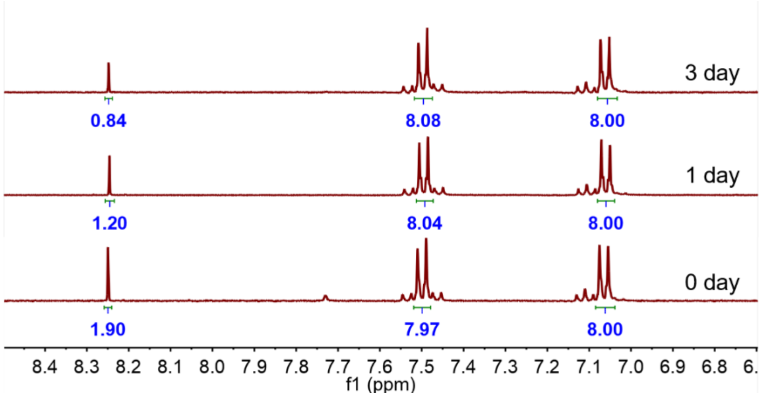

Figure S1. ^{1}H NMR spectrum after soaking in water of **NU-1008** in 0.1 M NaOD and diluted in D_2O formic acid vs Zr_6 = 1.68 vs 1 after soaking in water three days (original: formic acid vs Zr_6 = 3.80 vs 1)

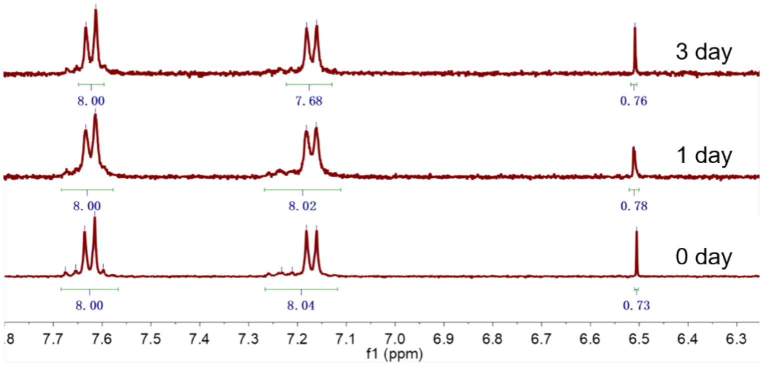

Figure S2. ^{1}H NMR spectrum after soaking in water of **NU-1008- FUM** digested in 0.1 M D_2SO_4 and diluted in d_6-DMSO. FUM vs Zr_6 = 0.76 vs 1 after soaking in water three days (original: FUM vs Zr_6 = 0.73 vs 1)

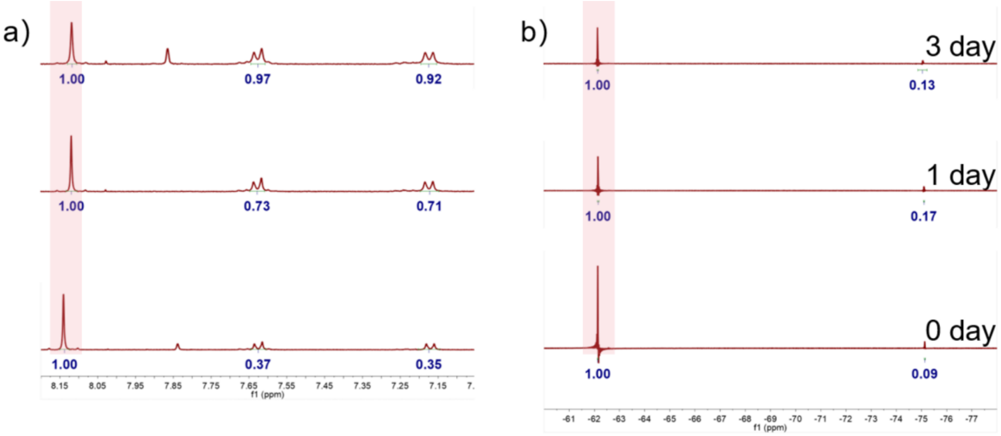

Figure S3. a) ^{1}H NMR spectrum after soaking in water of **NU-1008-TFA**/1,4-dibromo-2,5-bis(trifluoromethyl)benzene digested in 0.1 M D_2SO_4 and diluted in d_6-DMSO; b) ^{19}F NMR spectrum after soaking in water of **NU-1008-TFA**/1,4-dibromo-2,5-bis(trifluoromethyl)benzene digested in 0.1 M d_6-D_2SO_4 and diluted in DMSO. TFA vs Zr_6 = 2.14 vs 1 after soaking in water three days (original: TFA vs Zr_6 = 3.89 vs 1). 1,4-dibromo-2,5-bis(trifluoromethyl)benzene as the inner standard, highlighted in red and normalized to 1 in the spectra.

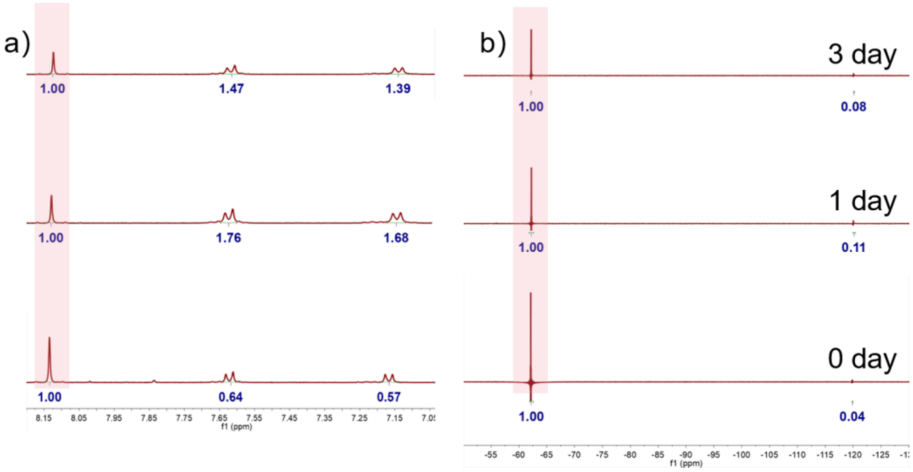

Figure S4. a) ^{1}H NMR spectrum after soaking in water of **NU-1008-TFS**/1,4-dibromo-2,5-bis(trifluoromethyl)benzene digested in 0.1 M D_2SO_4 and diluted in d_6-DMSO; b) ^{19}F NMR spectrum after soaking in water of **NU-1008 -TFS**/1,4-dibromo-2,5-bis(trifluoromethyl)benzene digested in 0.1 M d_6-D_2SO_4 and diluted in DMSO. TFS vs Zr_6 = 0.74 vs 1 after soaking in water three days (original: TFS vs Zr_6 = 0.74 vs 1). 1,4-dibromo-2,5-bis(trifluoromethyl)benzene as the inner standard, highlighted in red and normalized to 1 in the spectra.

4. Characterizations for NU-1008 analogues

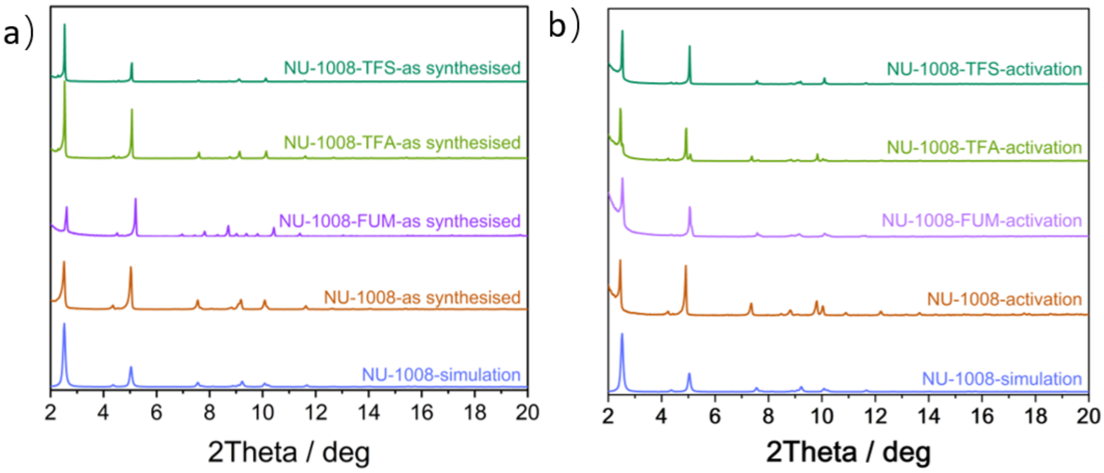

Figure S5. PXRD patterns of **NU-1008, NU-1008-FUM, NU-1008-TFA** and **NU-1008-TFS** (as synthesized samples (a), activated samples (b)).

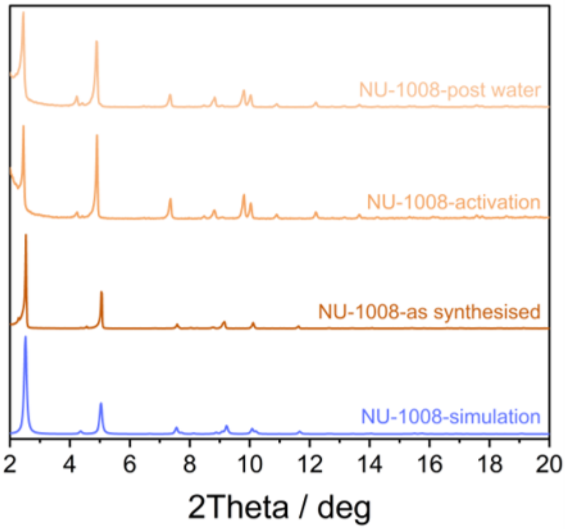

Figure S6. PXRD patterns for **NU-1008**.

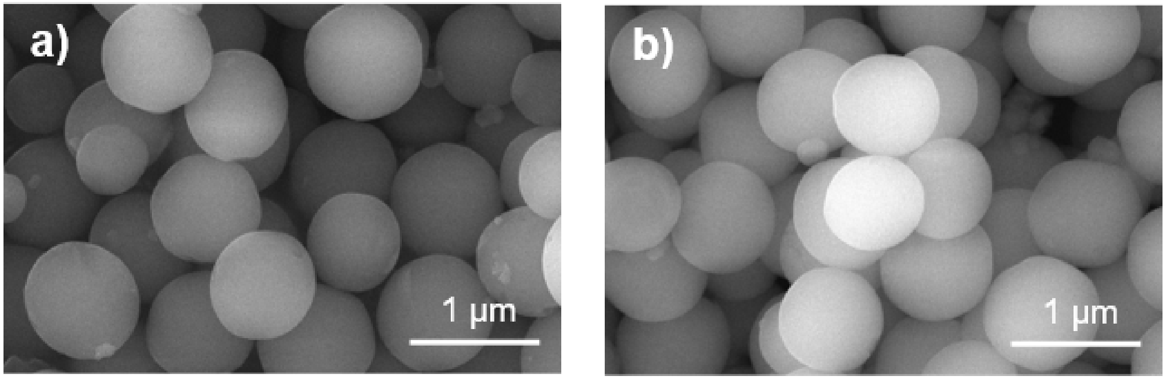

Figure S7. a) SEM image of **NU-1008**; b) SEM image of **NU-1008** after water-vapor cycle stability test.

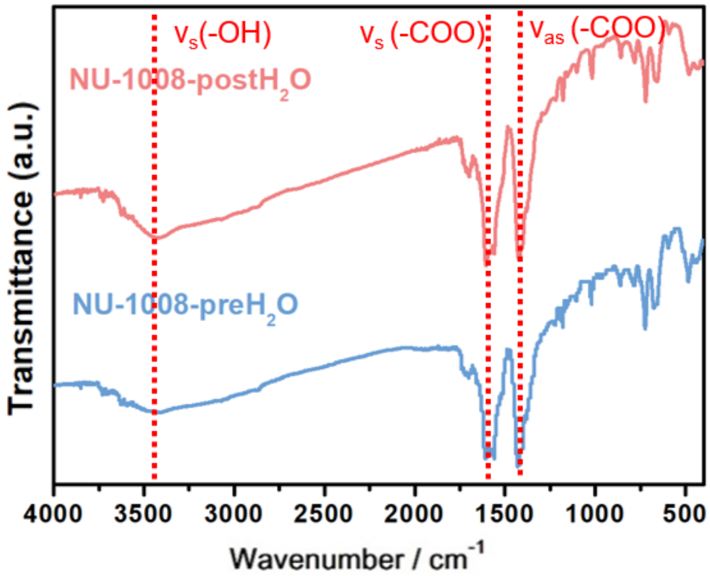

Figure S8. FT-IR spectra of **NU-1008** before and water cycling stability test.

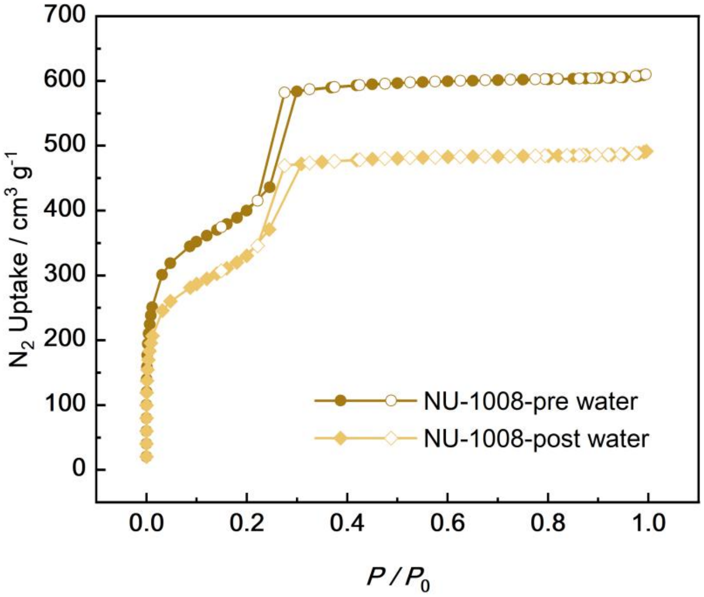

Figure S9. N_2 adsorption isotherms for **NU-1008** before and after water cycle stability test.

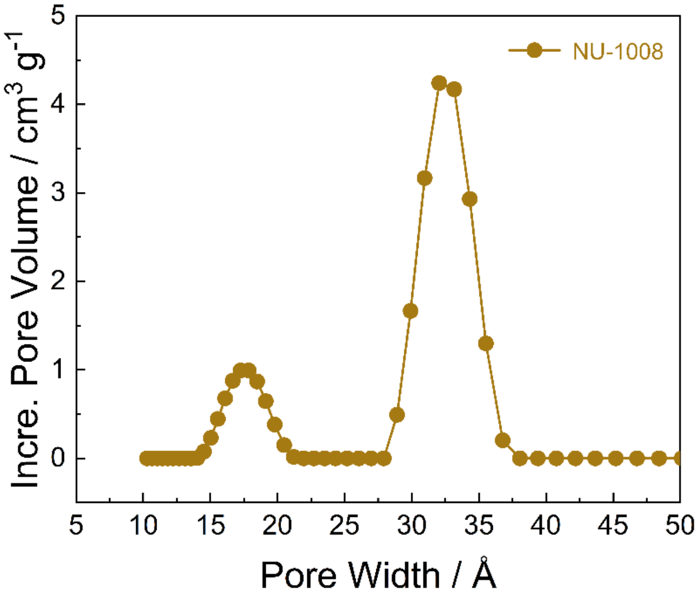

Figure S10. Pore size distribution of **NU-1008**.

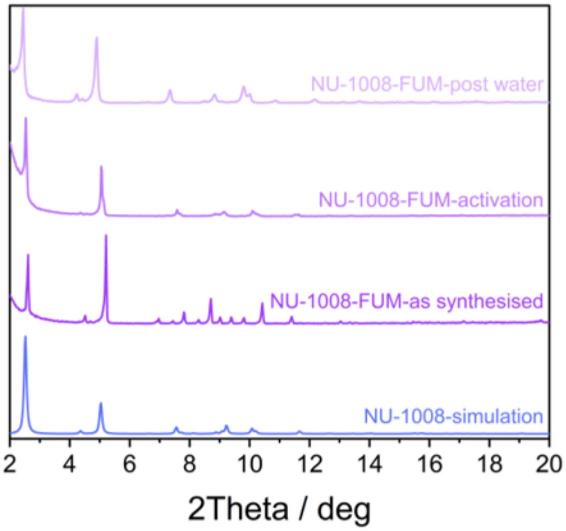

Figure S11. PXRD patterns of **NU-1008-FUM**.

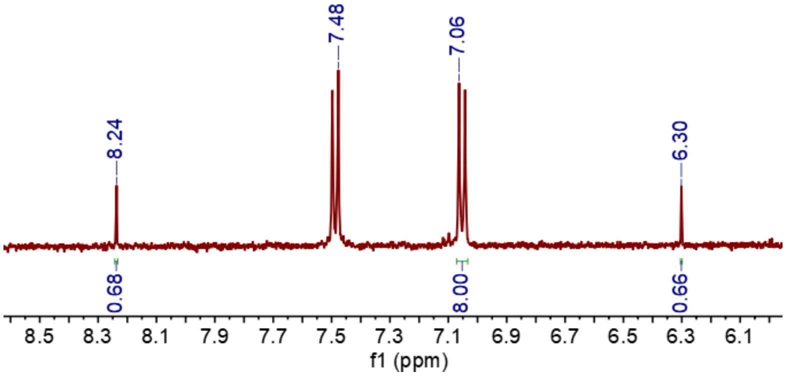

Figure S12. ^{1}H NMR spectrum of **NU-1008-FUM** digested in 0.1 M D_2SO_4 and diluted in d_6-DMSO. FUM vs Zr_6 = 0.7 vs 1 (theoretical: FUM vs Zr_6 = 1vs 1).

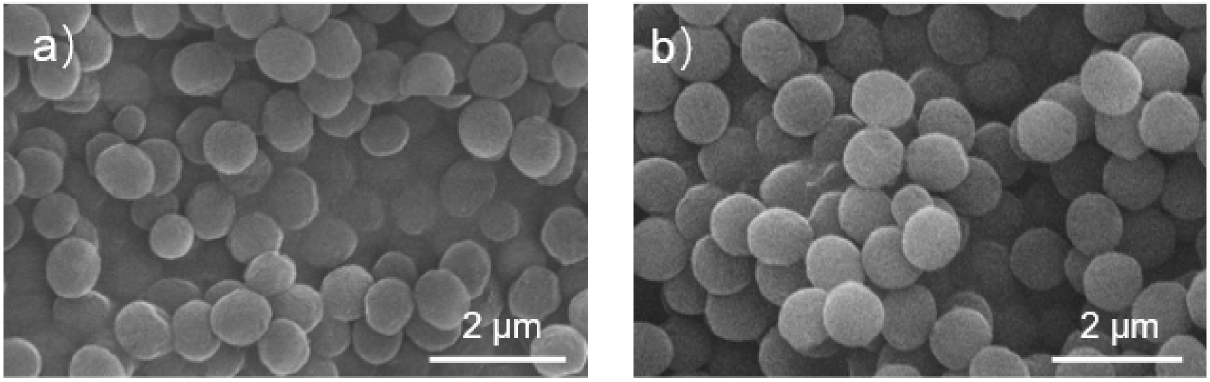

Figure S13. a) SEM image of **NU-1008-FUM**; b) SEM image of **NU-1008-FUM** after water-vapor cycle stability.

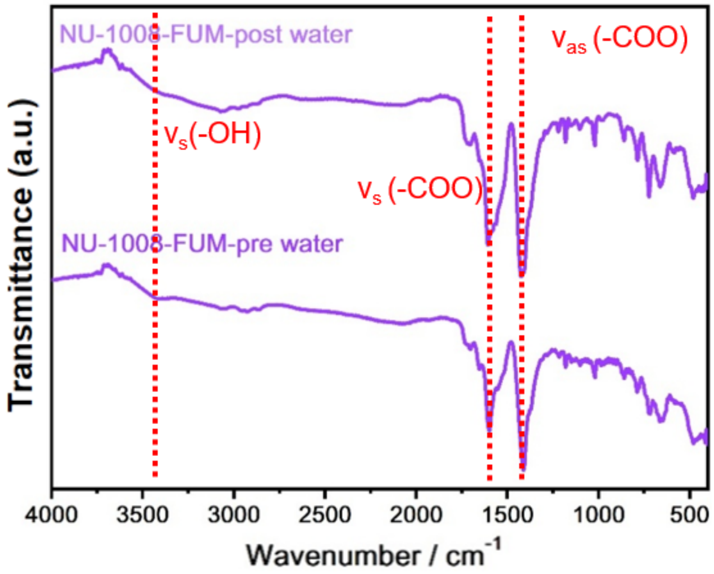

Figure S14. FT-IR spectra of **NU-1008-FUM** before and after water-vapor cycle stability test.

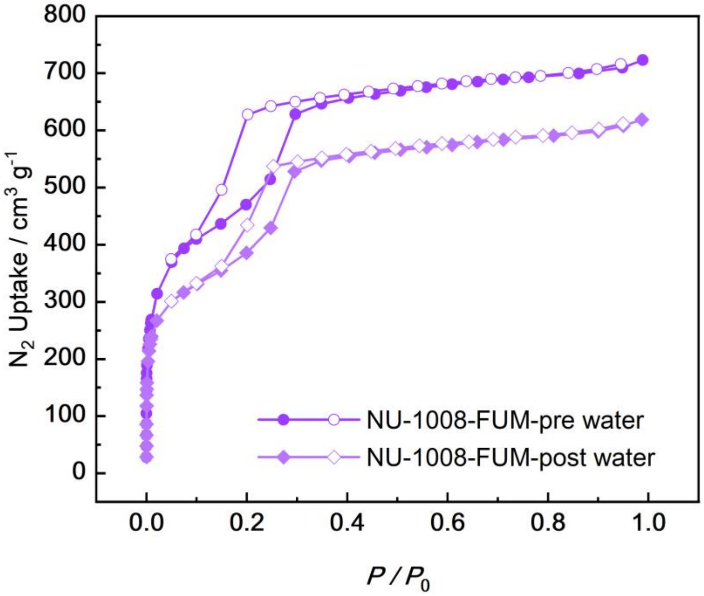

Figure S15. N_2 adsorption isotherms for **NU-1008-FUM** before and after water-vapor cycle stability test.

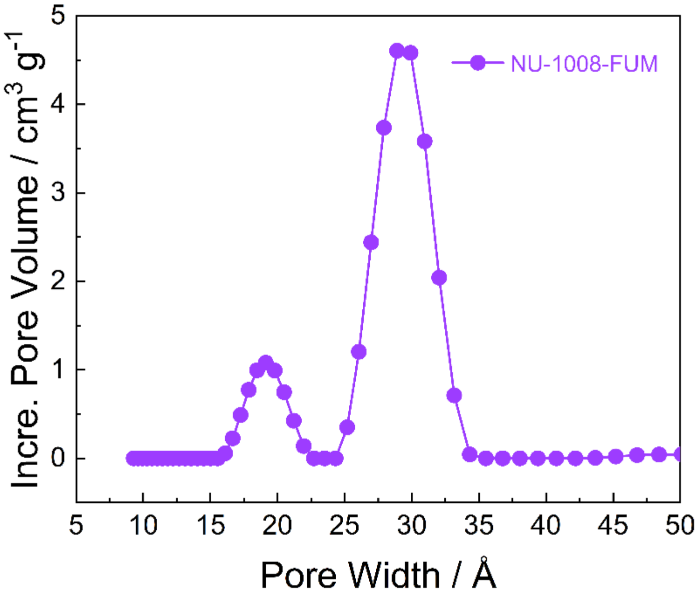

Figure S16. Pore size distribution of **NU-1008-FUM**.

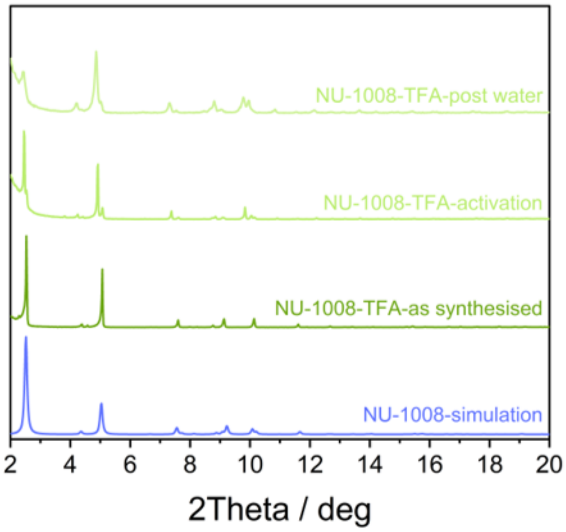

Figure S17. PXRD patterns of NU-1008-TFA.

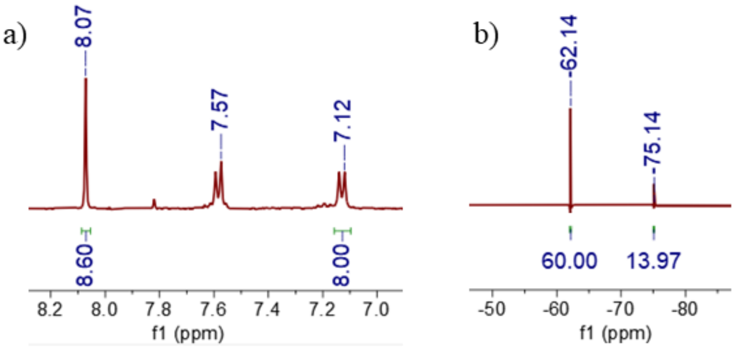

Figure 18. a) ^{1}H NMR spectrum of **NU-1008-TFA/**1,4-dibromo-2,5-bis(trifluoromethyl)benzene digested in 0.1 M D_2SO_4 and diluted in d_6-DMSO; b) ^{19}F NMR spectrum of **NU-1008-TFA/**1,4-dibromo-2,5-bis(trifluoromethyl)benzene digested in 0.1 M D_2SO_4 and diluted in d_6-DMSO. TFA vs Zr_6 = 4 vs 1(theoretical: TFA vs Zr_6 = 4 vs 1).

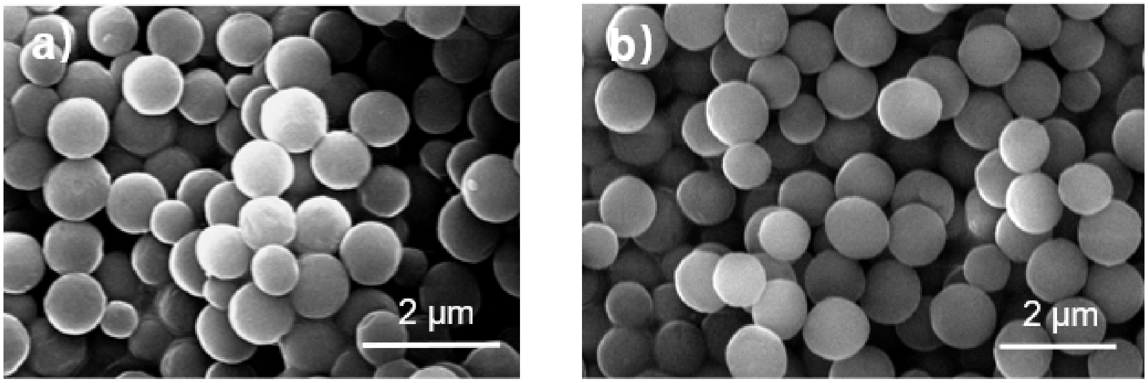

Figure S19. a) SEM image of **NU-1008-TFA**; b) SEM image of **NU-1008-TFA** after water-vapor cycle stability.

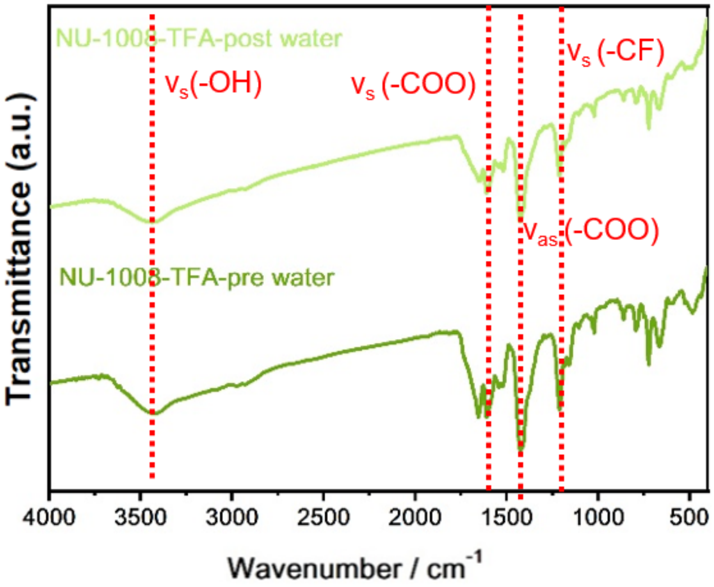

Figure S20. FT-IR spectra of **NU-1008-TFA** before and after water-vapor cycle stability test

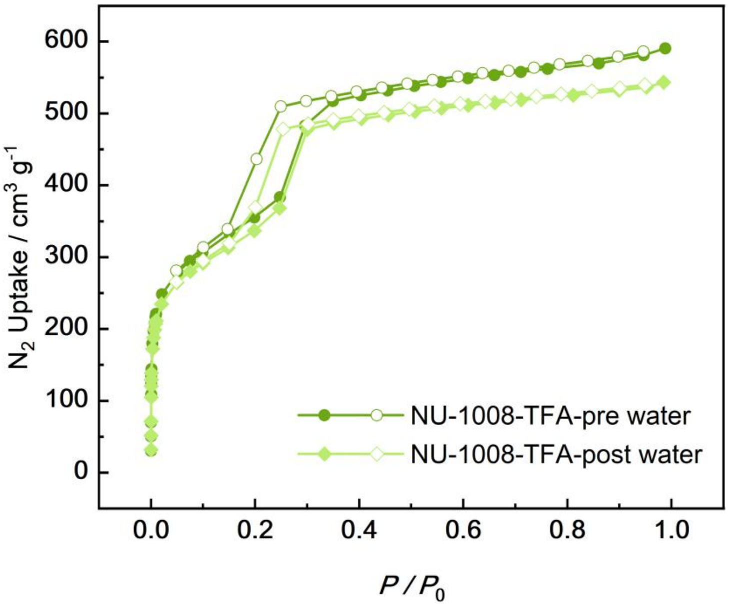

Figure S21. N_2 adsorption isotherms for **NU-1008-TFA** before and after water-vapor cycle stability test.

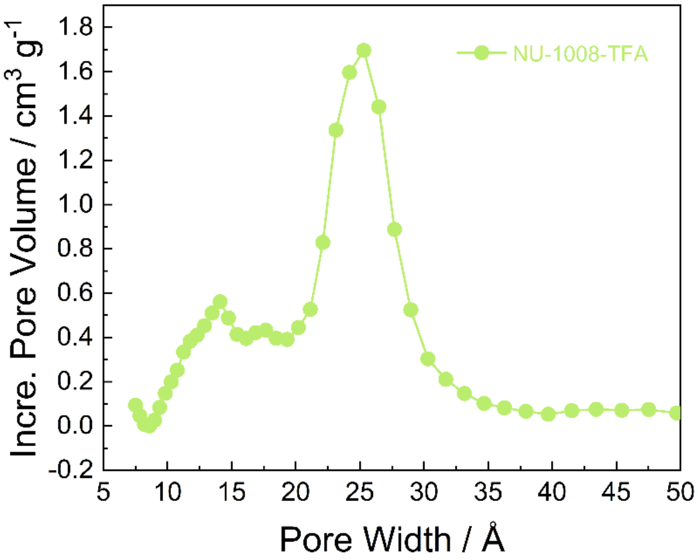

Figure S22. Pore size distribution of **NU-1008-TFA**.

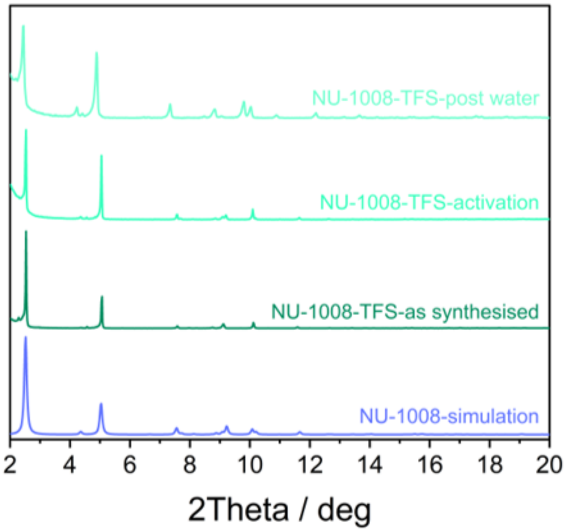

Figure S23. PXRD patterns of NU-1008-TFS.

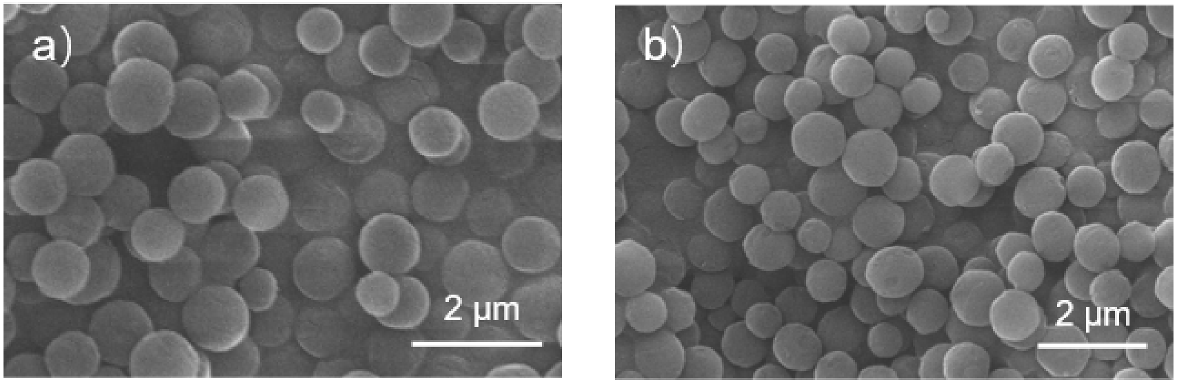

Figure S24. a) SEM image of **NU-1008-O-TFS**; b) SEM image of **NU-1008-O-TFS** after water-vapor cycle stability.

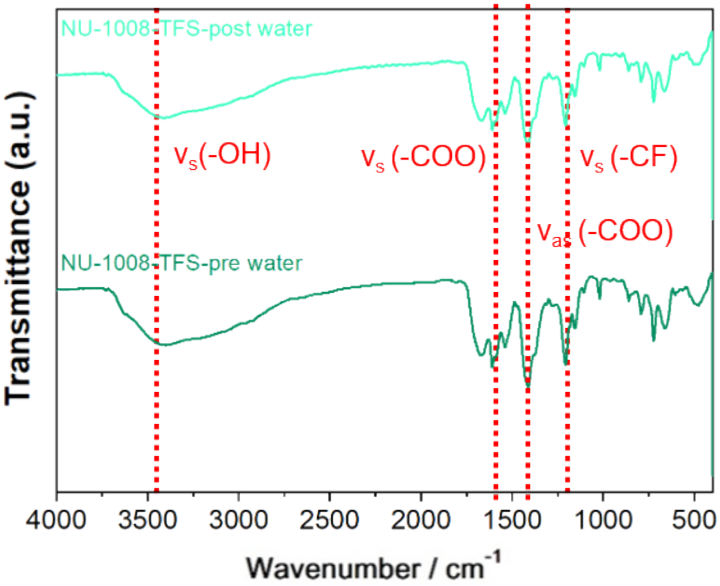

Figure S25. FT-IR spectra of **NU-1008-TFS** before and after water-vapor cycle stability test

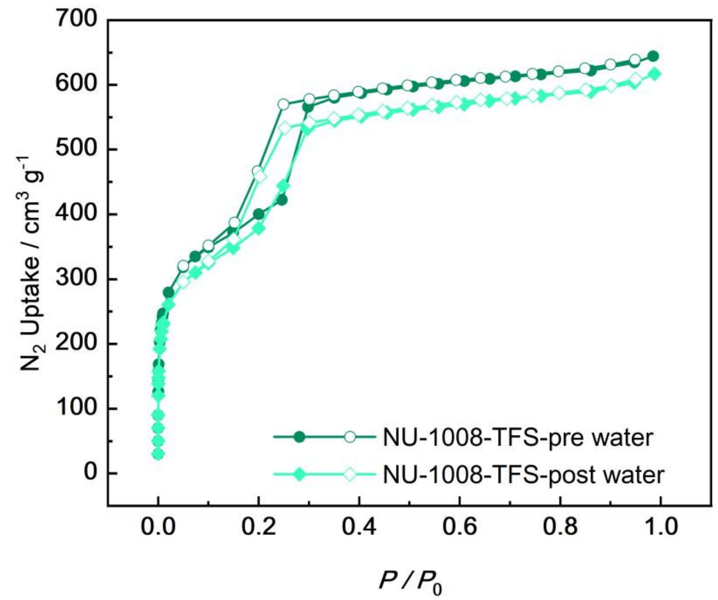

Figure S26. N$_2$ adsorption isotherms for **NU-1008-O-TFS** before and after water-vapor cycle stability test.

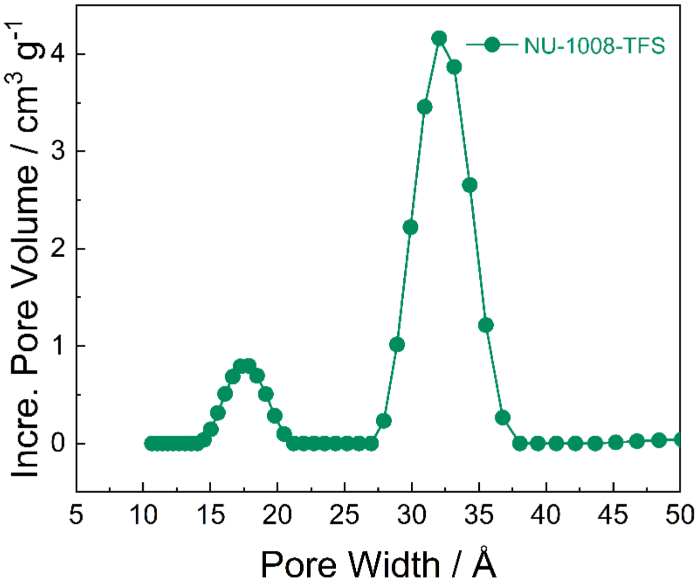

Figure S27. Pore size distribution of **NU-1008-TFS**.

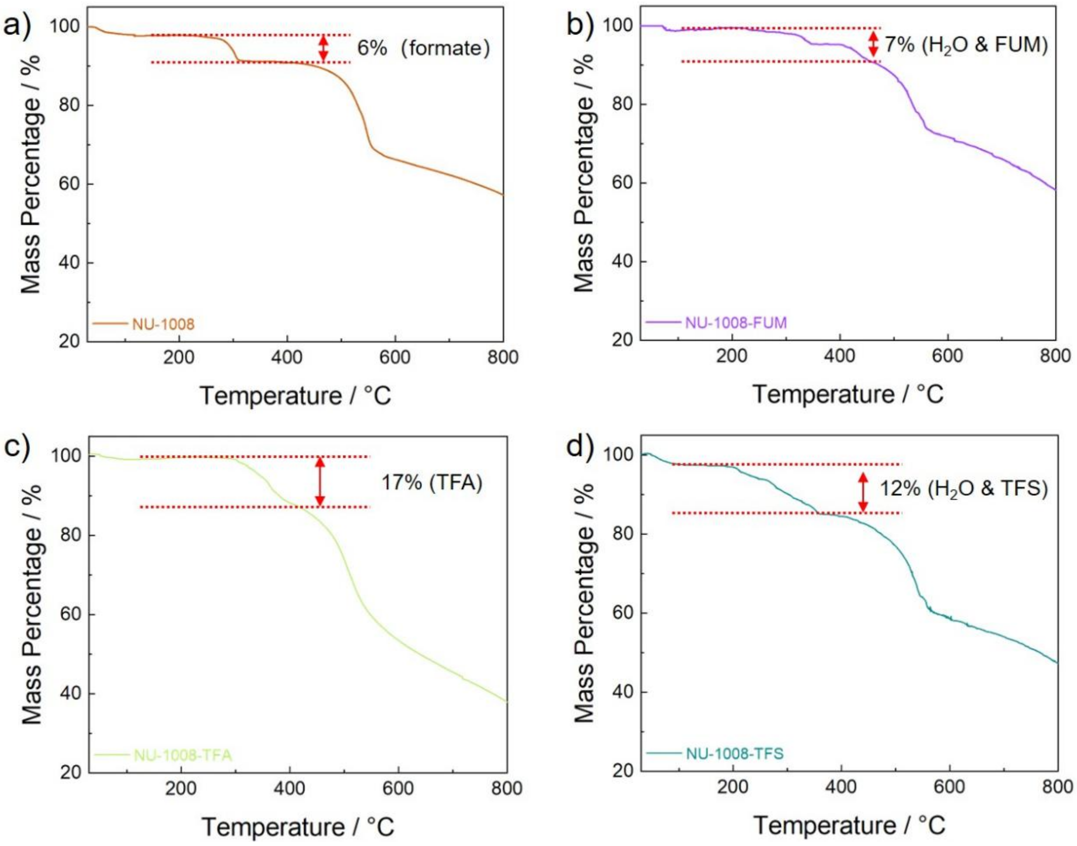

Figure S28. TG curves for NU-1008 (a), NU-1008-FUM (b), NU-1008-TFA (c), and NU-1008-TFS (d) under nitrogen atmosphere, respectively.

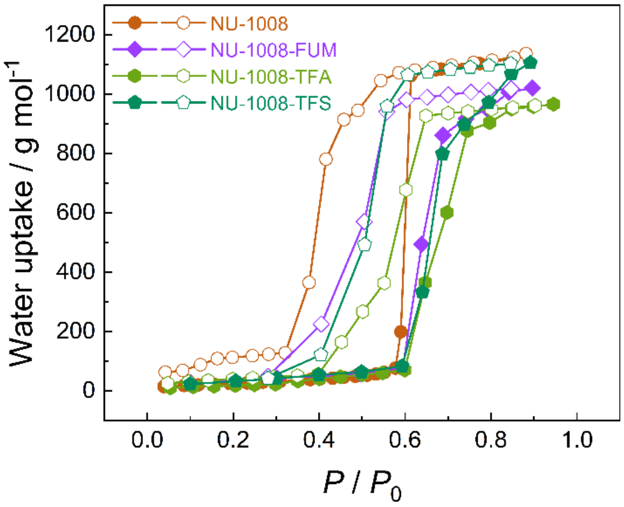

Figure S29. Water vapor adsorption isotherms measured at 298 K for NU-1008 analogues presented in the unit of g mol^{-1}.

5. Characterizations for NU-1008-TFS with different crystal dimensions

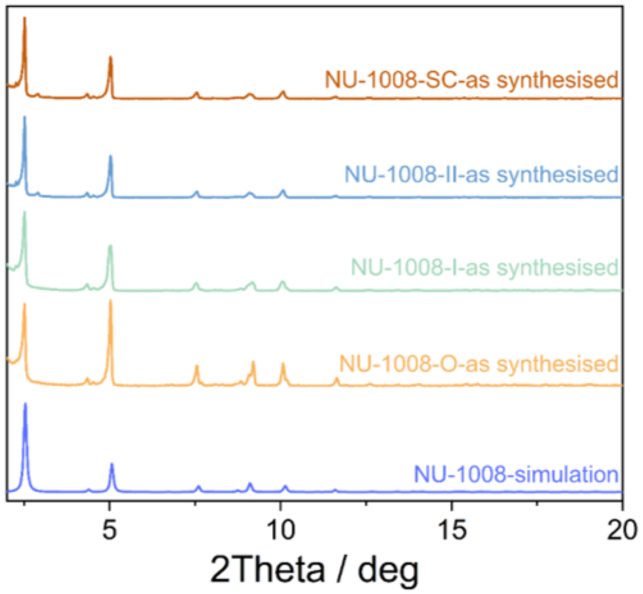

Figure S30. PXRD patterns of **NU-1008-O, NU-1008-I, NU-1008-II** and **NU-1008-SC**.

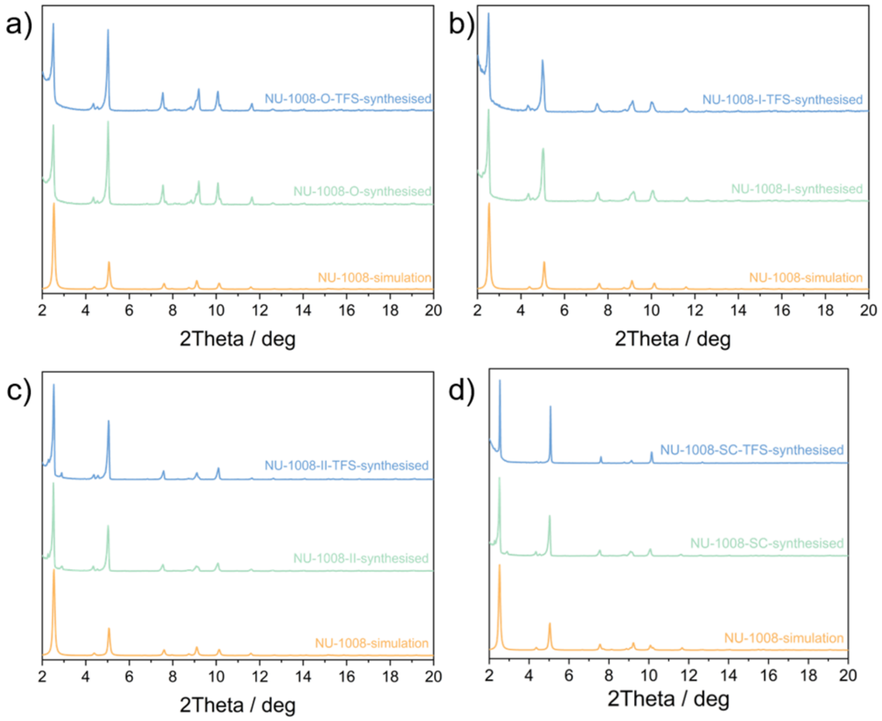

Figure S31. a) PXRD patterns of **NU-1008-O-TFS**; b) PXRD patterns of **NU-1008-I-TFS;** c) PXRD patterns of **NU-1008-II-TFS**; b) PXRD patterns of **NU-1008-SC-TFS.**

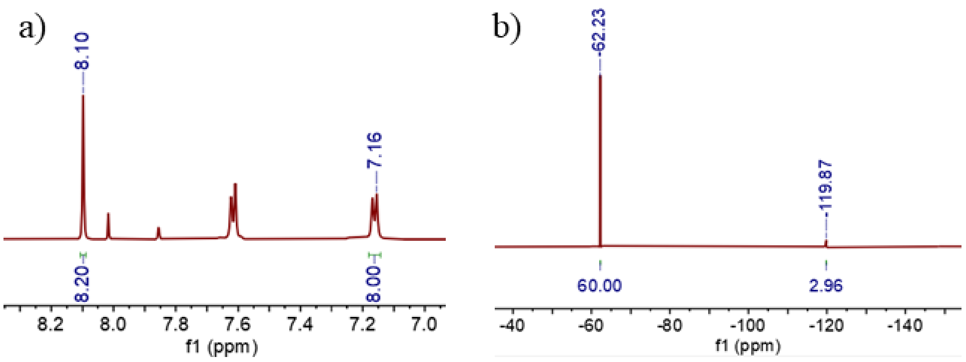

Figure S32. a) ^{1}H NMR spectrum of **NU-1008-O-TFS**/1,4-dibromo-2,5-bis(trifluoromethyl)benzene digested in 0.1 M D_2SO_4 and diluted in d_6-DMSO; b) ^{19}F NMR spectrum of **NU-1008-O-TFS**/1,4-dibromo-2,5-bis(trifluoromethyl)benzene digested in 0.1 M D_2SO_4 and diluted in d_6-DMSO. TFS vs Zr_6 = 0.81 vs 1(theoretical: TFS vs Zr_6 = 2 vs 1).

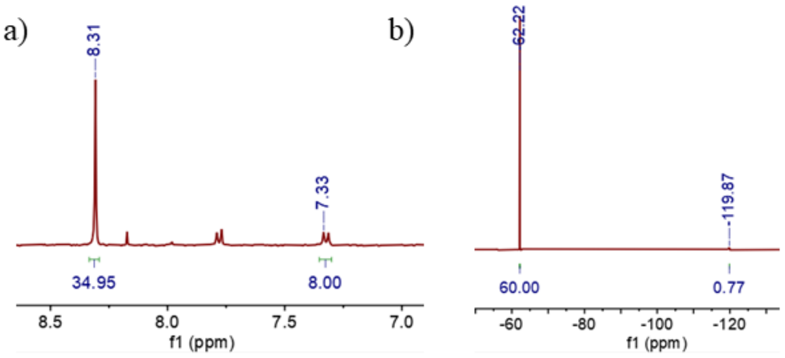

Figure S33. a) ^{1}H NMR spectrum of **NU-1008-I-TFS**/1,4-dibromo-2,5-bis(trifluoromethyl)benzene digested in 0.1 M D_2SO_4 and diluted in d_6-DMSO; b) ^{19}F NMR spectrum of **NU-1008-I-TFS**/1,4-dibromo-2,5-bis(trifluoromethyl)benzene digested in 0.1 M D_2SO_4 and diluted in d_6-DMSO. TFS vs Zr_6 = 0.90 vs 1(theoretical: TFS vs Zr_6 = 2 vs 1).

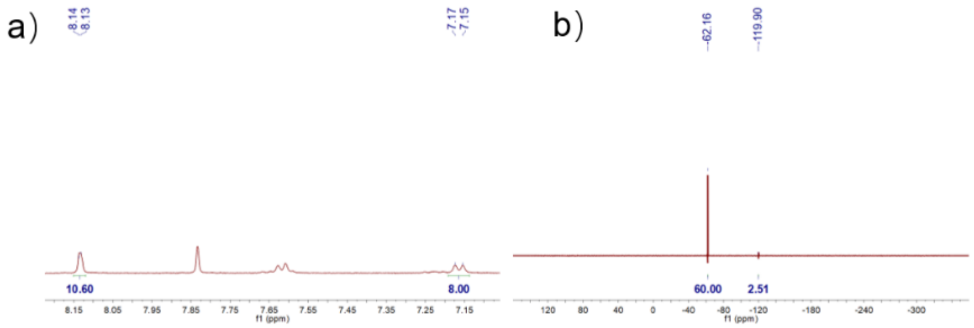

Figure S34. a) ^{1}H NMR spectrum of **NU-1008-II-TFS**/1,4-dibromo-2,5-bis(trifluoromethyl)benzene digested in 0.1 M D_2SO_4 and diluted in d_6-DMSO; b) ^{19}F NMR spectrum of **NU-1008-II-TFS**/1,4-dibromo-2,5-bis(trifluoromethyl)benzene digested in 0.1 M D_2SO_4 and diluted in d_6-DMSO. TFS vs Zr_6 = 0.88 vs 1(theoretical: TFS vs Zr_6 = 2 vs 1).

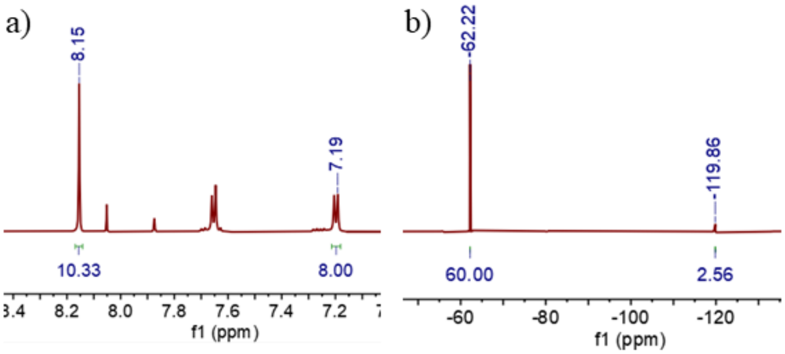

Figure S35. a) ^{1}H NMR spectrum of **NU-1008-SC-TFS**/1,4-dibromo-2,5-bis(trifluoromethyl)benzene digested in 0.1 M D_2SO_4 and diluted in d_6-DMSO; b) ^{19}F NMR spectrum of **NU-1008-SC-TFS**/1,4-dibromo-2,5-bis(trifluoromethyl)benzene digested in 0.1 M d_6-D_2SO_4 and diluted in DMSO. TFS vs Zr_6 = 0.88 vs 1(theoretical: TFS vs Zr_6 = 2 vs 1).

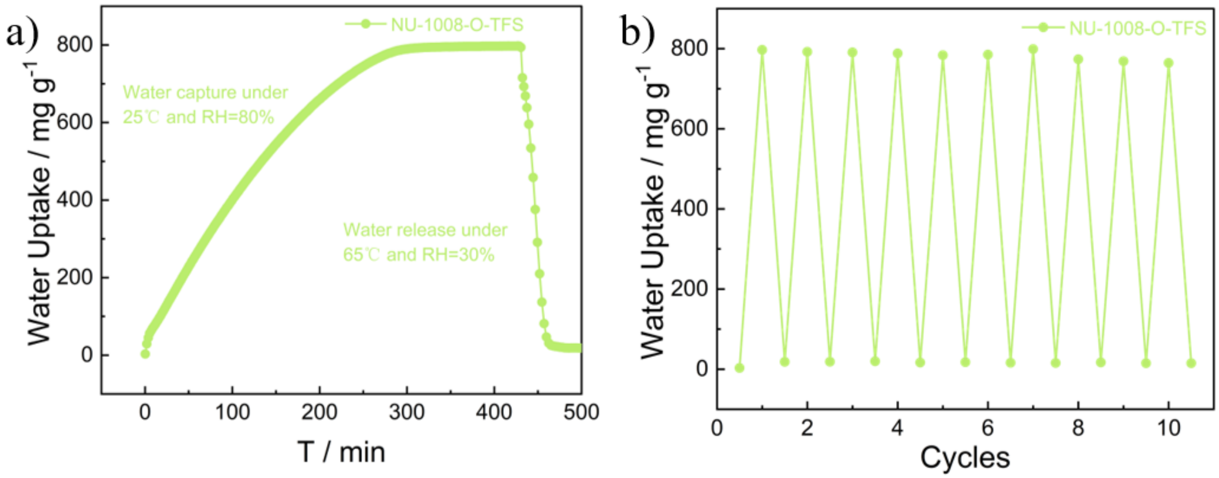

Figure S36. a) water adsorption kinetics for **NU-1008-O-TFS** (adsorption: 25 °C and 80% RH; desorption: 65 °C and 30% RH); b) ten-cycle stability test for **NU-1008-O-TFS**.

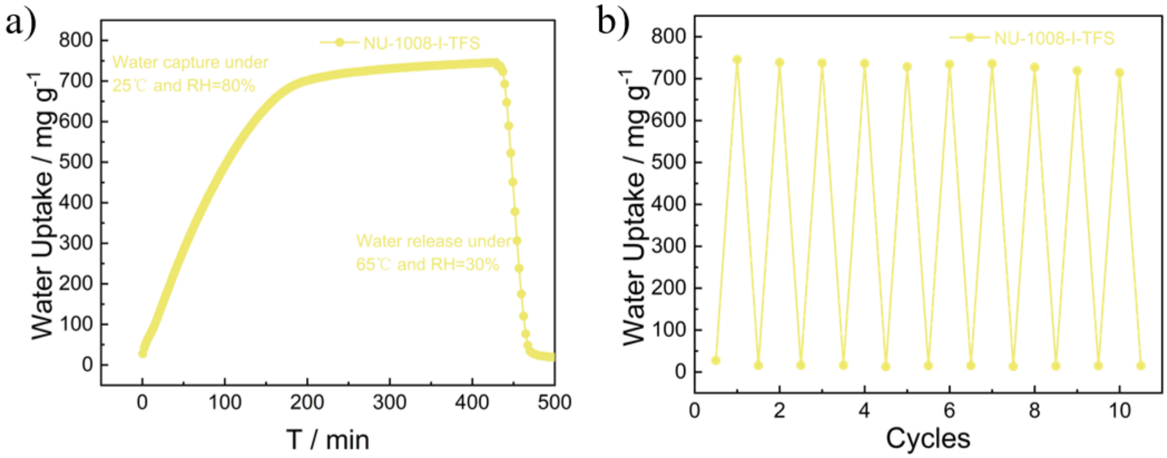

Figure S37. a) water adsorption kinetics for **NU-1008-I-TFS** (adsorption: 25 °C and 80% RH; desorption: 65 °C and 30% RH); b) ten-cycle stability test for **NU-1008-I-TFS**.

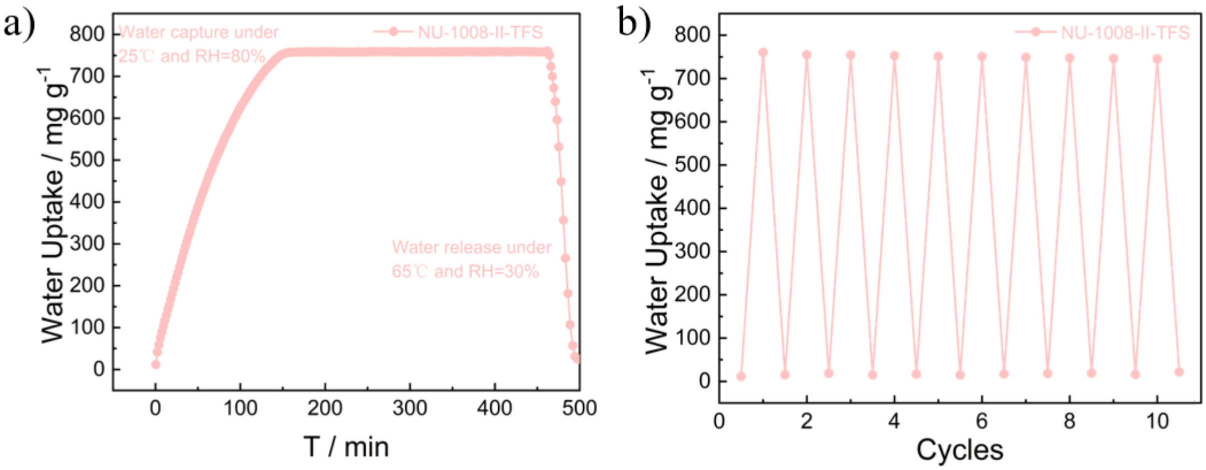

Figure S38. a) water adsorption kinetics for **NU-1008-II-TFS** (adsorption: 25 °C and 80% RH; desorption: 65 °C and 30% RH); b) ten-cycle stability test for **NU-1008-II-TFS**.

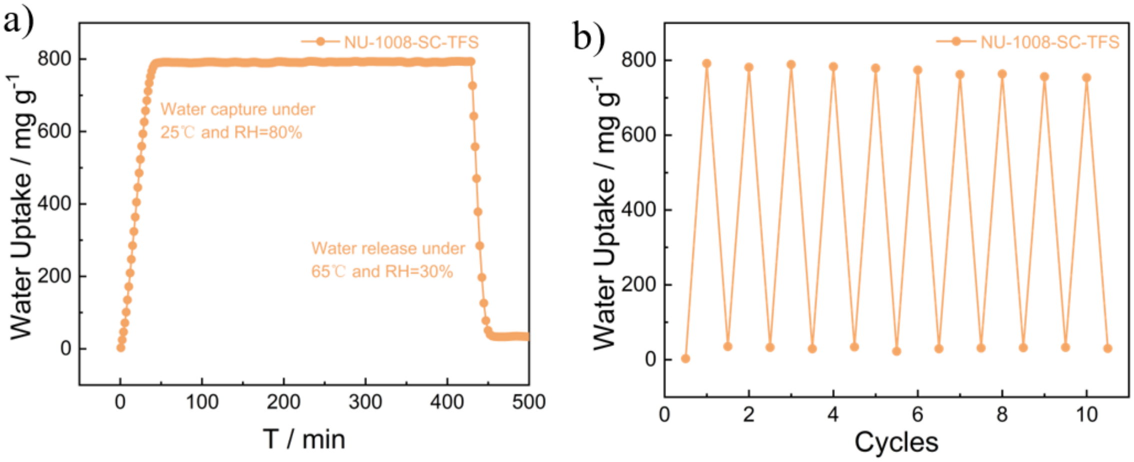

Figure S39. a) water adsorption kinetics for **NU-1008-SC-TFS** (adsorption: 25 °C and 80% RH; desorption: 65 °C and 30% RH); b) ten-cycle stability test for **NU-1008-SC-TFS**.

Table S2. Comparison of water adsorption capacity and adsorption rates for selected MOF materials

MOF	water adsorption capacity (g g^{-1})	adsorption rates (mg g^{-1} s^{-1})	RH (%)	References
NU-1008-0-TFS	0.8	0.044	80	This work
NU-1008-I-TFS	0.75	0.059	80	This work
NU-1008-II-TFS	0.76	0.083	80	This work
NU-1008-SC-TFS	0.8	0.34	80	This work
MOGs-6LiCl	1.05	0.058	80	[2]
UiO-66	0.4	0.016	40	[3]
CAU-10-H	0.58	0.02	60	[3]
MOF-801	0.5	0.023	50	[3]
MIL-101	1.27	0.042	70	[3]
UiO-66-NH2	0.38	0.29	70	[4]
MIL-125	0.22	0.14	70	[4]
Mil-125-NH2	0.4	0.14	70	[4]
MOF-808	0.7	0.79	70	[4]
Mg-SU-102	0.3	0.5	15	[5]

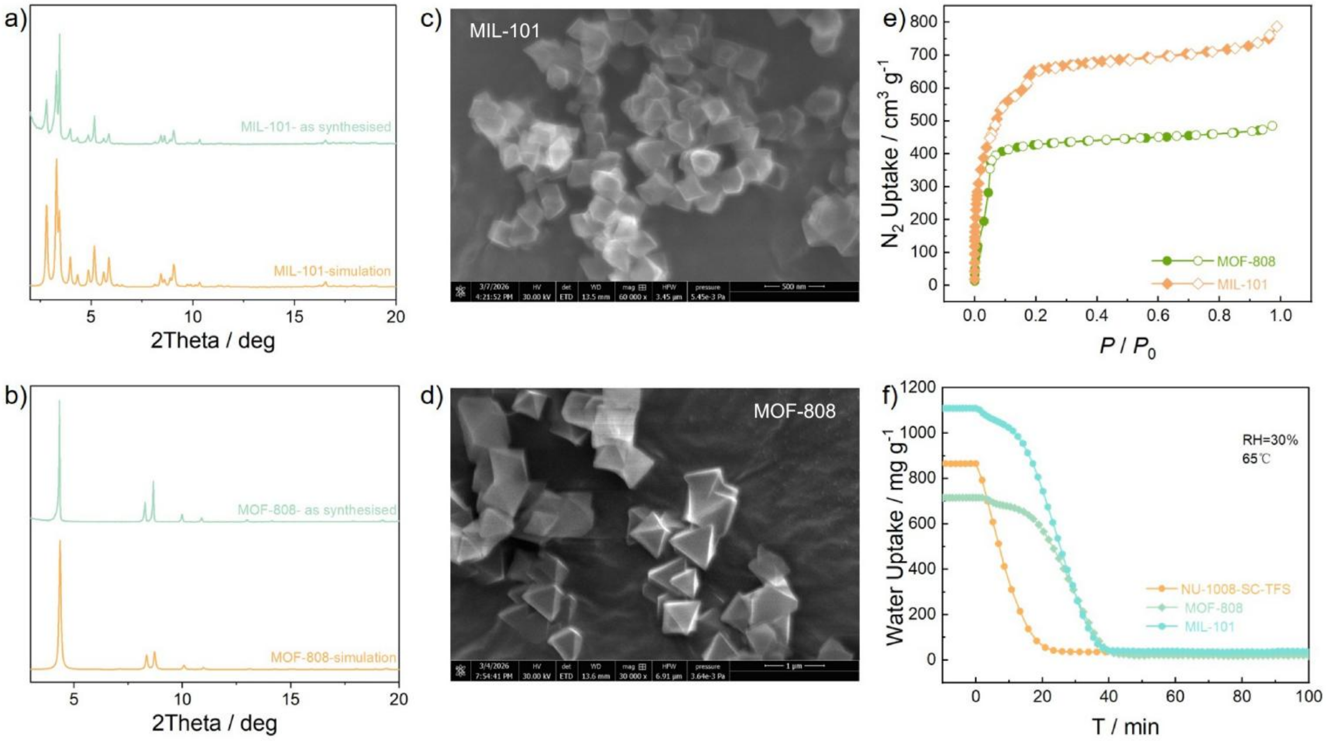

Figure S40. a) PXRD patterns for MIL-101(Cr); b) PXRD patterns for MOF-808; c) SEM image for MIL-101(Cr); d) SEM image for MOF-808; e) N_2 adsorption isotherms at 77 K for MIL-101(Cr) and MOF-808; f) the comparison of desorption kinetics for NU-1008-SC-TFS, MIL-101, and MOF-808 under similar operation condition.

1. References

[1] J. Lyu, X. Zhang, K.-i. Otake, X. Wang, P. Li, Z. Li, Z. Chen, Y. Zhang, M. C. Wasson, Y. Yang, P. Bai, X. Guo, T. Islamoglu and O. K. Farha, Chem. Sci., 2019, 10, 1186-1192.

https://doi.org/10.1039/c8sc04220a

[2] X. Zhou, G. Ma, W. Li, M. Cao, L. Nie, N. Han, J. Li, J. Gao, C. Yang, Y. Chen, "Biomimetic Super-Hygroscopic Metal–Organic Gel-Based Moisture Pump for Humidity Regulation," Advanced Functional Materials n/a (2025): e26552.

https://doi.org/10.1002/adfm.202526552

[3] C. Ma, J. Li, G. Wang, Z. Li, W. Su, Y. Zhou, "Microscopic Kinetics of Water Adsorption in Metal–Organic Frameworks." Nano Letters 25 (2025): 5778.

https://doi.org/10.1021/acs.nanolett.5c00343

[4] M. W. Logan, S. Langevin, Z. Xia, "Reversible Atmospheric Water Harvesting Using Metal-Organic Frameworks." Scientific Reports 10 (2020): 1492.

https://doi.org/10.1038/s41598-020-58405-9

[5] J. Oppenheim, Z. Yang, B. Dinakar, M. Dincă, "High-capacity water sorbent cycles without hysteresis under dry conditions," Nature Communications 16 (2025): 4297.

https://doi.org/10.1038/s41467-025-59551-2